We have interpreted the different relaxation energies, obtained for absorption into the exciton and A_{ab} state, as due to exciton screening of the core hole. The exciton wave function should therefore be localized primarily within one lattice spacing of the Mg ion. This is consistent with the size of the exciton determined through comparison of the exciton energy with the first allowed $2p^6 \rightarrow 2p^5 3s^1$ transition in gas phase Mg^{2+}. These transitions are within 0.15 eV of each other at room temperature,[11] suggesting that the spatial extent of the exciton is less than a lattice spacing. If the exciton were larger than a lattice spacing, the O^{2-} $2P$ states would screen the exciton, changing the energy from what is observed in the gas phase. The screening of the core hole potential by the exciton state is not complete, however. This is evident in the slight broadening with temperature of the exciton transition.

Phonon relaxation energies in ionic crystals have been estimated by Citrin, Eisenberger, and Hamann[3] (CEH) using polaron theory,[14] with reasonable success. Here the long-range Coulomb potential of the core hole is assumed to interact with the ionic polarizability of the lattice. The core hole potential interacts primarily with LO phonons. Due to the low dispersion of LO phonons, all phonons are considered to have the same frequency. In the strong-coupling limit,[14] assuming a Debye cutoff for the phonon wave vector, the relaxation energy is[3]

$$\Sigma_{ph} = e^2 (6/\pi V_m)^{1/2} (1/\epsilon_\infty - 1/\epsilon_0) , \qquad (2)$$

where V_m is the primitive cell volume, ϵ_∞ is the high-frequency dielectric constant (n^2), and ϵ_0 is the static dielectric constant. For MgO we obtain $\Sigma_{ph} = 1.6$ eV. This should be compared with our measured value of $\Sigma_{ph} = 2.1$ eV for absorption into state A_{ab} (ionized core hole). This is consistent with the trend found by CEH when comparing their results on alkali halides to this model; the model underestimates the relaxation energy. More recently, Mahan has obtained closer fits to the available alkali halide data using a multimode model. In his analysis, Mahan[4] determined that LO phonons at X provide the important temperature dependence to the linewidth. We are not aware of any such calculations on MgO although Mahan's model, which considers localized holes in a point-ion lattice, should be applicable for MgO.

Similar measurements were made on α-Al_2O_3 and α-SiO_2. Shown in Fig. 3 are the room-temperature SXE/E^3 and SXA spectra for α-Al_2O_3 and α-SiO_2. Relaxation energies were determined for the VBE and exciton transitions for α-Al_2O_3. These relaxation energies are reported in Table I. The relaxation energy for the exciton transition, 0.4 eV, is less than the relaxation energy for the VBE transition, 1.6 eV. This is similar to what was found for MgO and suggests that the Al L exciton is localized primarily within a nearest-neighbor distance. No changes were observed in either the SXE or SXA spectra of α-SiO_2 over the temperature range studied, 300–1000 K. The large experimental upper limit in Σ_{ph} for the VBE transition, 1.0 eV, is due to the broad shape of the α-SiO_2 VBE.

The temperature dependence of the electronic transition energies for MgO are presented in Fig. 4. Here the transition energies are shown relative to the $T = 300$ K values, so that all the information can be contained on one graph. As the temperature increases, the VBM and the A_{em} feature move to higher energies, while the exciton moves to lower energies. We detect no shift for the $2P \rightarrow 2S$ transition or the A_{ab} and B_{ab} features. These transitions are omitted from Fig. 4 for brevity. The results presented in Fig. 4 were fit with a linear least-squares routine. The temperature coefficients are presented in Table II. Similar measurements were made on α-Al_2O_3 and α-SiO_2. Linear temperature coefficients for the transitions identified in Fig. 3 are presented in Table II. For α-Al_2O_3 the VBM and other emission features move to higher energies with an increase in temperature while the exciton moves to lower energies. We observe no temperature-dependent shift in the α-SiO_2 SXE and SXA spectra. The absence of a temperature-dependent shift can be ex-

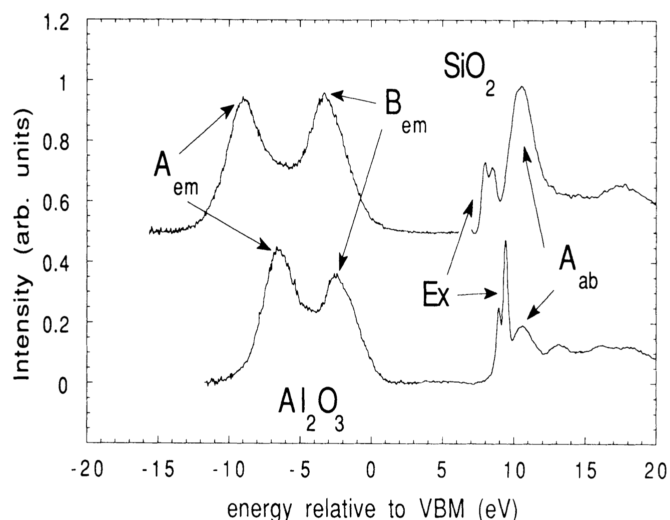

FIG. 3. Room-temperature SXE/E^3 and SXA of α-SiO_2 (top) and α-Al_2O_3 (bottom). The relaxation energies and temperature coefficients for the electronic transitions identified are listed in Tables I and II, respectively.

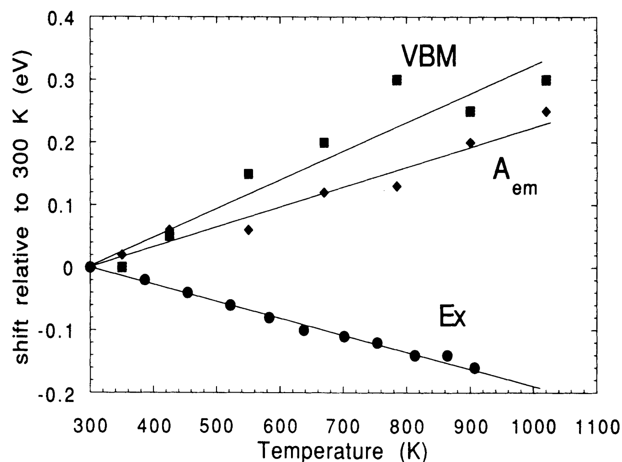

FIG. 4. Temperature dependence of VBM (■), A_{em} (♦), and Ex (●) transition energies of MgO. Transition energies are shown relative to their values at 300 K.

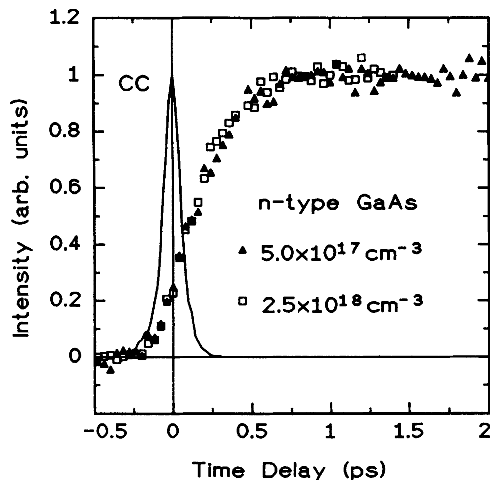

FIG. 1. Temporal evolution of the band-edge luminescence of *n*-doped GaAs at two different doping levels. The cross-correlation of laser and scattered light (CC) determines zero delay and demonstrates the time resolution of the experiment.

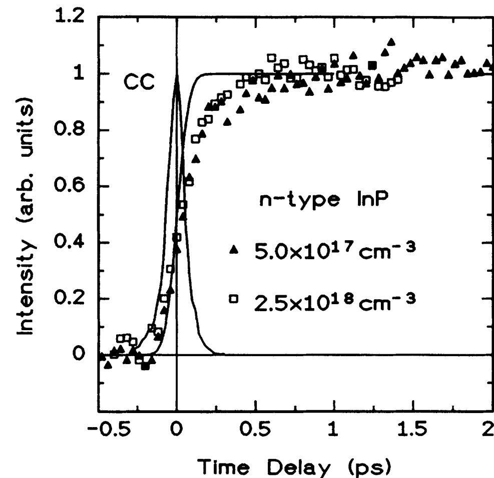

FIG. 2. Temporal evolution of the band-edge luminescence of *n*-doped InP at two different doping levels. The solid line indicates the electron-hole plasma density generated in the sample.

carrier recombination and diffusion. At both doping levels, the signal has reached already 30% of the maximum intensity during the optical excitation ($\Delta t = 0$ fs), implying a large spectral broadening of excited holes down to the band edge in less than 50 fs. The signal maximum is reached 700 fs after excitation. Any further significant relaxation of the holes would lead a change in the band-edge signal. We therefore conclude that the thermal equilibrium between excited holes and lattice has to be established in about 700 fs in GaAs at 300 K at a hole density of 5×10^{16} cm^{-3}.[15] The rise times for different doping densities shown in Fig. 1 imply that the energy relaxation of holes does not depend on the concentration of electrons. This indicates that intrinsic relaxation processes in the valence bands dominate the electron-hole interaction in the energy relaxation of holes.

Figure 2 shows the time evolution of the BE signal in *n*-type InP at two different doping levels. The results are similar to those for GaAs. Note that the rise is not limited by the temporal resolution of our up-conversion system. The BE signal reaches 45% of the maximum intensity during the optical excitation ($\Delta t = 0$ fs) and rises considerably faster than in the case of *n*-type GaAs. In the first 150 fs, 80% of the maximum signal is already reached. This reveals a strong coupling of hot holes to the lattice in InP. Thereafter the slope levels off, reaching the maximum after 400 fs. Thermal equilibrium with the lattice is thus established in this time. Similar to GaAs, the rise time also does not depend on electron density in the range from 5×10^{17} to 5×10^{18} cm^{-3}.

For a quantitative discussion of our results, we have to consider electron-hole energy transfer and relaxation via emission of optical phonons (LO and TO). Relaxation via acoustic phonons can be neglected, because the average kinetic energy of optically excited holes is greater than the optical-phonon energy in our room-temperature experiment. The experimentally measured doping independence of the BE luminescence rise behavior indicates already a negligible role of *e-h* energy transfer in the hole energy relaxation. After a simple plasma theory for the nondegenerate case,[16] the energy transfer from hot holes to a cold electron plasma with $n = 5\times10^{17}$ cm^{-3} is estimated to be on the order of 0.2 eV/ps for both GaAs and InP. This computed rate is much too small to explain the femtosecond hole relaxation observed here. Based on the experimentally observed doping independence and this theoretical estimate, we assume that electron-hole scattering is not the dominating scattering mechanism for the hole relaxation. One caveat about this assumption is that the observed doping independence of the experimental rise time might also be partly explained by the degeneracy of the electron system: For higher doping densities, the degeneracy leads to a reduction of *e-h* collision probability. Similar to the reduced momentum relaxation rate with increasing carrier density,[17] the energy-transfer rate between electrons and holes might not increase any more with increasing doping.

In a first step, we model the experimental data by calculating the cooling of an internally thermalized plasma due to polar-optical emission of LO phonons. We consider as a first approximation an isotropic parabolic valence-band structure. The different valence-band symmetry is taken into account by using a correction factor with a value of 2.[18] Based on the measured instantaneous spectral spreading of hole distributions, we assume an instantaneous hole thermalization among the three valence bands in our calculations. Such an ultrafast internal thermalization of holes has previously been observed by Knox *et al.*[3] The initial hole temperature is determined by the hole excess energy during the excitation. In the whole calculation, intervalence-band relaxation is also neglected. The calculated curves (Figs. 3 and 4) for *polar-optical scattering* have a rise significantly too slow to explain the experimental results in both materials, although all assumptions should lead to an enhanced rise time of the band-edge signal. Hence, the ultrafast hole relaxation found in experiments has to be attributed to a strong optical deformation-potential coupling. The quantitative role of this effect estimated in previous works is widely

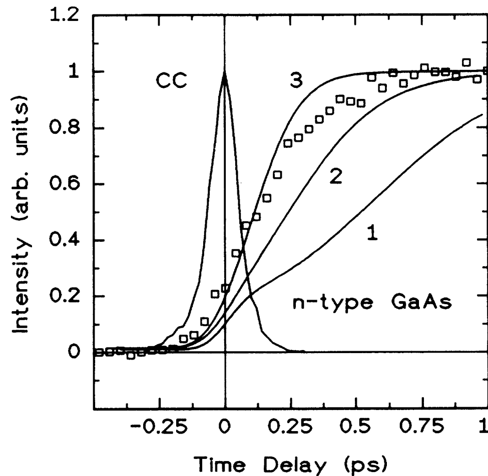

FIG. 3. Comparison of the time-resolved band-edge luminescence of n-type GaAs between experimental data (squares) and calculations including (1) only LO phonon emission, (2) LO+TO phonon emission with $E_{\mathrm{NOD}}=10$ eV; and (3) LO+TO phonon emission with $E_{\mathrm{NOD}}=25$ eV.

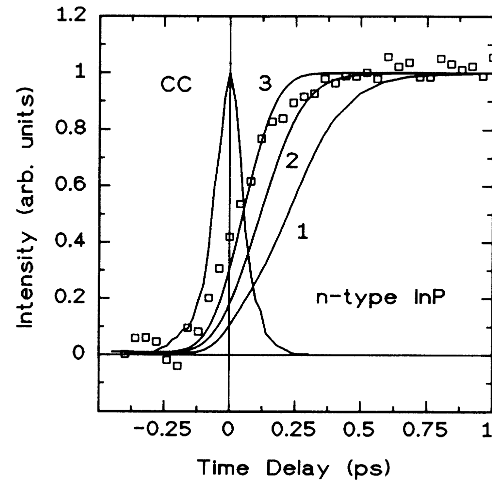

FIG. 4. Comparison of the time-resolved band-edge luminescence of n-type InP between experimental data (squares, $N_D=2.5\times10^{18}$ cm^{-3}) and calculations including (1) only LO phonon emission, (2) LO+TO phonon emission with $E_{\mathrm{NOD}}=10$ eV, and (3) LO+TO phonon emission with $E_{\mathrm{NOD}}=30$ eV.

different, with deformation-potential constants E_{NOD} varying from 10 (Ref. 11) to 41 eV.[12]

In a second step, we fit the cooling of the internally thermalized holes including deformation-potential coupling[19] and the LO-phonon emission described above. As shown in Figs. 3 and 4, best fits are obtained with $E_{\mathrm{NOD}}=25(^{+10}_{-5})$ eV for GaAs and 30($\pm$10) eV for InP, respectively. The corresponding maximal total energy-loss rate in the initial relaxation with a photon energy of 2 eV is on the order of 1.0 eV/ps for GaAs and 2.0 eV/ps for InP. A small deviation between our model and the experimental data in InP and particularly GaAs indicate the limit of our model for a quantitative evaluation. Possible explanations are the finite lifetime of holes in the split-off band, which slows down the total hole relaxation rate. Another explanation is a dependence of the optical deformation potentials on the k vector,[20] which could slow down the cooling close to the band edge. Detailed theoretical models including these effects are needed for a complete understanding of the ultrafast hole relaxation.

In conclusion, we have studied the ultrafast hole relaxation in bulk GaAs and InP at room temperature. In n-doped compounds, the hole thermal equilibrium with the lattice is completed after 400 to 700 fs for an optical excitation of 2 eV. The dominant energy-loss channel of holes is attributed to optical deformation-potential coupling.

We thank S. Zollner for discussions about deformation potentials, W. Rühle for a critical reading of the manuscript, M. Maassen for supplying a variety of samples, U. Lemmer for the collaboration in numerical calculations, and R. Kersting and H. Mikkelsen for technical assistance in building the up-conversion setup. This work has been supported by the Deutsche Forschungsgemeinschaft (Ku 540/3) and by the Alfried Krupp Stiftung.

*Present address: Max-Planck-Institut für Festkörperforschung, W-7000 Stuttgart 80, Germany.

[1]R. F. Leheny, J. Shah, R. L. Fork, and C. V. Shank, Solid State Commun. **31**, 809 (1979).

[2]W. H. Knox, M. C. Downer, R. L. Fork, and C. V. Shank, Opt. Lett. **9**, 150 (1984).

[3]W. H. Knox, D. S. Chemla, G. Livescu, J. Cunningham, and J. E. Henry, Phys. Rev. Lett. **61**, 1290 (1988).

[4]X. Q. Zhou, G. C. Cho, U. Lemmer, W. Kütt, K. Wolter, and H. Kurz, Solid-State Electron. **32**, 1591 (1989); X. Q. Zhou, U. Lemmer, K. Seibert, G. C. Cho, W. Kütt, K. Wolter, and H. Kurz, Proc. SPIE Int. Soc. Opt. Eng. **1268**, 166 (1990).

[5]T. Elsaesser, J. Shah, L. Rota, and P. Lugli, Phys. Rev. Lett. **66**, 1757 (1991).

[6]For bulk GaAs, see, e.g., S. Lyon, J. Lumin. **35**, 121 (1986); for quantum wells, see J. Shah, A. Pinczuk, A. C. Gossard, and W. Wiegmann, Phys. Rev. Lett. **54**, 2045 (1985); or K. Leo, W. W. Rühle, and K. Ploog, Phys. Rev. B **38**, 1947 (1988).

[7]J. Shah, B. Deveaud, T. C. Damen, W. T. Tsang, A. C. Gossard, and P. Lugli, Phys. Rev. Lett. **59**, 2222 (1987).

[8]P. C. Becker, H. L. Fragnito, C. H. Brito-Cruz, J. Shah, R. L. Fork, J. E. Cunningham, J. E. Henry, and C. V. Shank, Appl. Phys. Lett. **53**, 2089 (1988).

[9]A. J. Taylor, D. J. Erskine, and C. L. Tang, J. Opt. Soc. Am. B **2**, 663 (1985).

[10]*Properties of GaAs*, 2nd ed. (Institute of Electrical Engineers, London, 1990).

[11]M. Pugnet, J. Collet, and A. Cornet, Solid State Commun. **38**, 531 (1981).

[12]W. Pötz and P. Kocevar, Phys. Rev. B **28**, 7040 (1983).

[13]J. Shah, IEEE J. Quantum Electron. **QE-22**, 1728 (1986).

[14]X. Q. Zhou, Ph.D. thesis, Technical University of Aachen, 1991 (unpublished).

[15]The maximum intensity of BE signal increases only slightly (less than a factor of 2) for the two doping densities shown here. The signal even decreases by more than a factor of 10

when the doping density is increased from 2.5×10^{18} cm^{-3} to a few times 10^{19} cm^{-3}.

[16] R. A. Höpfel and J. Shah, Phys. Rev. Lett. **56**, 765 (1986).
[17] M. Combescot and R. Combescot, Phys. Rev. B **35**, 7986 (1987).
[18] E. O. Göbel and O. Hildebrand, Phys. Status Solidi B **88**, 645 (1978).
[19] E. M. Conwell, *High Field Transport in Semiconductors* (Academic, New York, 1967); T. Brudevoll, T. A. Fjeldly, J. Baek, and M. S. Shur, J. Appl. Phys. **67**, 7373 (1990).
[20] S. Zollner, S. Gopalan, M. Garriga, J. Humlicek, L. Vina, and M. Cardona, Appl. Phys. Lett. **57**, 2838 (1990); S. Zollner, S. Gopalan, and M. Cardona, J. Appl. Phys. **68**, 1682 (1990).